AIP | APL Materials

Reduced graphene oxide wrapped Cu2O supported on C3N4: An efficient visible light responsive semiconductor photocatalyst

S. Ganesh Babu, R. Vinoth, P. Surya Narayana, Detlef Bahnemann, and B. Neppolian

Citation: APL Mater. **3**, 104415 (2015); doi: 10.1063/1.4928286
View online: http://dx.doi.org/10.1063/1.4928286
View Table of Contents: http://scitation.aip.org/content/aip/journal/aplmater/3/10?ver=pdfcov
Published by the AIP Publishing

Reduced graphene oxide wrapped Cu_2O supported on C_3N_4: An efficient visible light responsive semiconductor photocatalyst

S. Ganesh Babu,[1] R. Vinoth,[1] P. Surya Narayana,[1] Detlef Bahnemann,[2] and B. Neppolian[1,a]
[1]*SRM Research Institute, SRM University, Kattankulathur, Chennai 603203, India*
[2]*Institute of Technical Chemistry, Leibniz University of Hannover, D-30167 Hannover, Germany*

(Received 29 April 2015; accepted 26 July 2015; published online 25 August 2015)

Herein, Cu_2O spheres were prepared and encapsulated with reduced graphene oxide (rGO). The Cu_2O–rGO–C_3N_4 composite covered the whole solar spectrum with significant absorption intensity. rGO wrapped Cu_2O loading caused a red shift in the absorption with respect to considering the absorption of bare C_3N_4. The photoluminescence study confirms that rGO exploited as an electron transport layer at the interface of Cu_2O and C_3N_4 heterojunction. Utmost, ~2 fold synergistic effect was achieved with Cu_2O–rGO–C_3N_4 for the photocatalytic reduction of 4-nitrophenol to 4-aminophenol in comparison with Cu_2O–rGO and C_3N_4. The Cu_2O–rGO–C_3N_4 photocatalyst was reused for four times without loss in its activity. [http://dx.doi.org/10.1063/1.4928286]

Semiconductor photocatalysis technique is one of the best environmental friendly methods for the degradation of organic pollutants, removal of heavy metals, water purification, and disinfection.[1–3] Owing to the non-toxicity, chemical stability, insolubility in water, and the favorable optical property, titania (TiO_2) is regarded as the promising material to approach the universal energy and environmental crises.[4,5] Unfortunately, TiO_2 can only be excited by ultraviolet (UV) light, which limits its application to a great extend.[6] Many approaches have been proposed to make the TiO_2 as visible light active: metal ion implanted TiO_2, reduced TiO_x photocatalysts, non-metal doped TiO_2, composites of TiO_2 with semiconductor having lower band gap energy, sensitizing of TiO_2 with dyes, and TiO_2 with luminescence agent.[7–12] On the other hand, a great research effort is being taken to replace the UV light active TiO_2 photocatalyst with the visible light active stable photocatalysts. Recently, Wang *et al.* reported a novel metal free polymer material and graphitic carbon nitride (g-C_3N_4) for the production of H_2 by splitting of water via photocatalysis.[13] Because of its lower band gap energy, g-C_3N_4 (E_g = 2.7 eV) can absorb natural sunlight and thereby active under visible light. More interestingly, C_3N_4 possesses more favorable properties to be a suitable photocatalyst such as extremely thermally stable, chemically inert, and resistive towards photocorrosion.[14] High recombination rate of electron-hole pairs makes the pristine C_3N_4 to be less efficient under visible light irradiation that limits its energy and environmental applications. Furthermore, C_3N_4 suffers with inadequate photon absorption capability after ~460 nm.[15] Many methods have been developed to overcome the above two demerits such as doping of metals or non-metals and combining with graphene.[16,17] Hence, to make the C_3N_4 photocatalyst more efficient, copper(I) oxide (Cu_2O) is deposited on the surface of C_3N_4. It is well known that Cu_2O is a promising visible light active photocatalyst due to its low band gap energy (2.2 eV), nontoxicity, and natural abundance.[18] For example, Tion *et al.* reported the preparation of C_3N_4/Cu_2O heterojunction and its photocatalytic studies for the degradation of methyl orange dye under visible light irradiation.[19]

[a]Author to whom correspondence should be addressed. Electronic mail: neppolian.b@res.srmuniv.ac.in

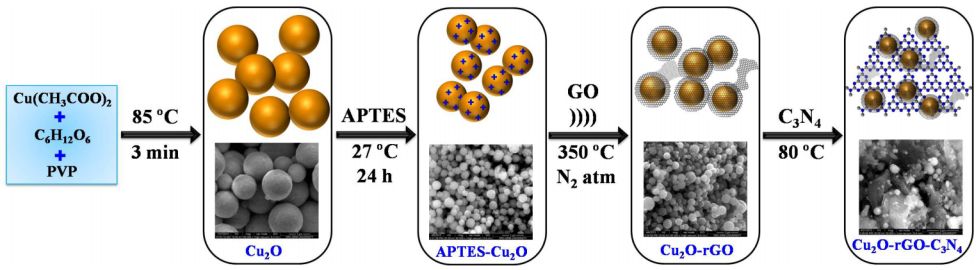

FIG. 1. Schematic illustration for the preparation of Cu_2O–rGO–C_3N_4 photocatalyst.

To enhance the reactivity of the photocatalyst or to reduce the charged carrier recombination, rGO was used as a potential carbonaceous solid support in many of the photocatalytic systems.[20] But insertion of the rGO exactly at the interfacial of the two heterojunction is another key challenge. Hence, in this particular research work, Cu_2O spheres were wrapped with rGO layer and then deposited on the surface of C_3N_4, so that the rGO layers are precisely in between the p-n heterojunction of Cu_2O and C_3N_4. So, rGO effectively increased the charged carrier mobility in the interfacial region of the two semiconducting materials. To prove the efficacy of the prepared composite, photocatalytic reduction of 4-nitrophenol was performed under visible light irradiation which is an important organic reaction as per industrial perspective.

The schematic representation for the preparation of Cu_2O–rGO–C_3N_4 photocatalyst is illustrated in Figure 1. Cu_2O spheres were prepared by simple wet solution method using $Cu(CH_3COO)_2 \cdot H_2O$, glucose, and polyvinyl pyrolidone. The as-prepared Cu_2O spheres were characterized by scanning electron microscope - energy dispersive spectroscopy (SEM-EDS) analysis. As depicted in Figure 2(a), the Cu_2O possesses exact spherical in shape. This hierarchical spherical structure made the wrapping of rGO extremely straightforward. More importantly, no defective spots were identified in the spherical structure which emphasized the reliability of this preparation protocol [Figures 2(b)-2(d)]. Furthermore, the purity of the sample was estimated by EDS analysis which confirmed the presence of Cu and O (the elemental C peak came from double side carbon tape used as a sample holder for SEM-EDS measurements) [Figure 2(e)]. In order to find the phase purity of the prepared Cu_2O spheres, XRD analysis was carried out and the pattern exactly resembled the XRD pattern of Cu_2O (JCPDS card number is 77-0199).[21] More importantly, no peaks were observed with respect to the CuO, which confirmed the complete reduction of Cu^{2+} ($Cu(CH_3COO)_2 \cdot H_2O$) to Cu^{+} (Cu_2O) [Figure 2(f)].[22]

XRD patterns of Cu_2O, (3-Aminopropyl)triethoxysilane (APTES) modified Cu_2O, Cu_2O–rGO, Cu_2O–rGO–C_3N_4 and C_3N_4 are depicted in Figure 3. As discussed previously, the XRD peaks of phase pure primitive lattice Cu_2O spheres were observed. The XRD pattern of surface modified Cu_2O using APTES precisely resembled with the pure Cu_2O spheres that revealed that surface modification only generated positive charges on the surface of Cu_2O spheres but not created any changes in the phases and oxidation states. However, while wrapping the rGO layer onto the surface of Cu_2O spheres, a new XRD peak centered at $2\theta = 38.74°$ was appeared, corresponding to the (111) plane of CuO.[23,24] This oxidation of Cu_2O to CuO occurred during the calcination process. Nevertheless, the intensity of the peak was very less which authenticated that the over-oxidation was very minimal because the calcination performed under inert condition (in presence of N_2 atmosphere). It is worth to mention here that no authenticated peaks were observed for rGO in the XRD spectra of both Cu_2O–rGO and Cu_2O–rGO–C_3N_4 photocatalysts which might be due to the lowest loading of GO (1%). The additional two peaks in the XRD pattern of Cu_2O–rGO–C_3N_4 photocatalyst at 13.05° and 27.55° were corresponded to the (001) and (002) planes of graphitic C_3N_4 (g-C_3N_4), respectively.[25] This was further confirmed by comparing the XRD spectrum of bare g-C_3N_4 as shown in Figure 3.

Figure 4 represents the SEM images of APTES modified Cu_2O, Cu_2O–rGO and Cu_2O–rGO–C_3N_4 photocatalysts. It is seen that APTES not only created positive charges on the surface of Cu_2O spheres but also reduced the particle size which is clearly evident from the SEM images of

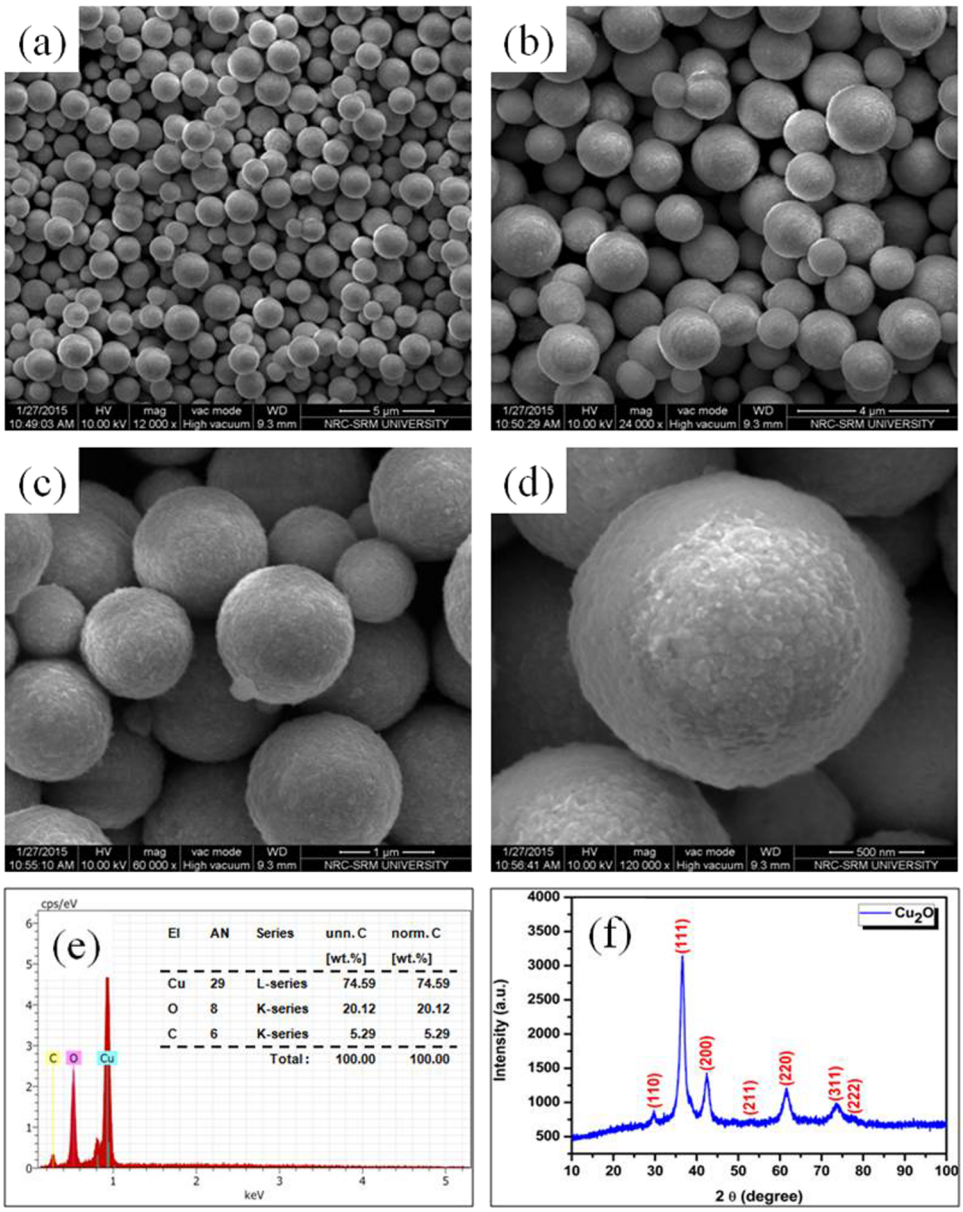

FIG. 2. (a)-(d) SEM images of hierarchically structured Cu_2O spheres with different magnifications. (e) EDX graph [inset: elemental wt. % table] and (f) XRD pattern of Cu_2O spheres.

APTES modified Cu_2O [Figures 4(a) and 4(b)]. This size contraction might be due to the existence of more positive charges on the surface of Cu_2O. Presence of rGO layer in Cu_2O–rGO photocatalyst was verified by the SEM images as shown in Figure 4(c). Complete wrapping of rGO over Cu_2O spheres were confirmed from the Figure 4(d). Nonetheless, only a meager amount of free rGO layers were identified at the background which authenticated the complete utilization of rGO for the wrapping of Cu_2O spheres.[26] The SEM images of Cu_2O-rGO-C_3N_4 composite are depicted in Figures 4(e) and 4(f). In addition, even after introducing C_3N_4, the spherical morphology of Cu_2O was maintained. Furthermore, the SEM results revealed that the rGO wrapped Cu_2O spheres were dispersed homogeneously on the surface of C_3N_4.

In order to understand the absorption behavior and band gap of Cu_2O, C_3N_4 and Cu_2O–rGO–C_3N_4, ultraviolet-visible (UV-vis) spectroscopy was studied in diffused reflectance spectroscopy (DRS) mode. The results are shown in Figure 5. The absorption range was restricted to 460 and

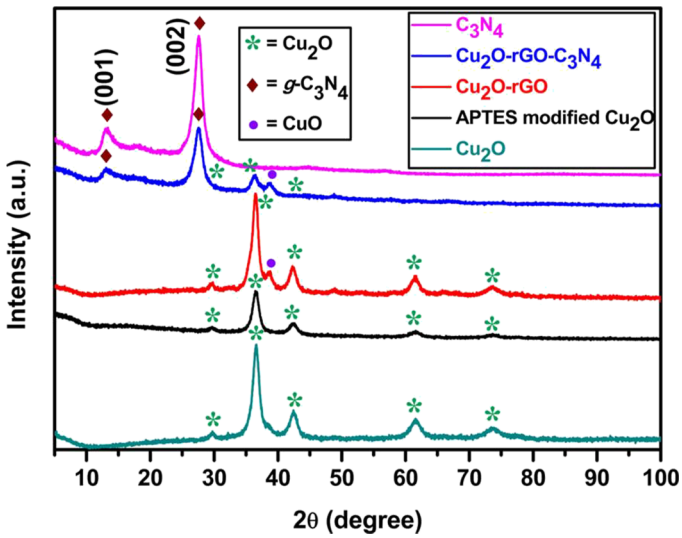

FIG. 3. XRD patterns of Cu_2O, APTES modified Cu_2O, Cu_2O–rGO, Cu_2O–rGO–C_3N_4, and C_3N_4.

600 nm for pristine Cu_2O and C_3N_4, respectively, which was in good agreement with the literature reports.[27,28] But the Cu_2O–rGO–C_3N_4 composite covered almost the whole solar spectrum that favors the material to be photoactive [Figure S1(a) in the supplementary material].[36] The absorption intensity was also remarkably increased after loading Cu_2O–rGO to C_3N_4 and appeared as a red shift in comparison with bare C_3N_4. The adsorption edge of pristine C_3N_4 was 450 nm which can be assigned to the band gap energy of 2.75 eV [Figure S1(b) in the supplementary material].[36] Bare Cu_2O possesses the band gap energy of 2.20 eV [Figure S1(c) in the supplementary material].[36] Similarly, the absorption edge of Cu_2O–rGO–C_3N_4 photocatalyst was about 477 nm and the calculated band gap was 2.60 eV [Figure S1(d) in the supplementary material].[29,36]

Photoluminesence (PL) spectroscopy is one of the powerful tools to examine the charge transfer, migration, and extend of separation in photocatalysts. Figure 5 shows the PL spectra of pure C_3N_4, Cu_2O, Cu_2O–rGO, and Cu_2O–rGO–C_3N_4 photocatalysts. In the PL spectrum of pristine C_3N_4, a peak centered at 450 nm, corresponding to the band gap of C_3N_4.[29] The other three materials, namely, Cu_2O, Cu_2O–rGO, and Cu_2O–rGO–C_3N_4 showed broad PL emission peak from 500 to 700 nm. Very importantly, the peak intensity at this region was in the order of Cu_2O > Cu_2O–rGO > Cu_2O–rGO–C_3N_4 which confirmed that the charged carriers recombination was very high in pristine Cu_2O. It is well known fact that rGO has higher carrier mobility and thereby reduced the recombination rate in Cu_2O–rGO photocatalyst. As a result, the peak intensity was lesser for Cu_2O–rGO than bare Cu_2O. But the peak intensity was decreased further by adding C_3N_4 to Cu_2O–rGO. It is worth to mention here that the Cu_2O–rGO–C_3N_4 photocatalyst showed two PL emission peaks at around 500 to 700 nm and 450 nm which were emerged because of Cu_2O and C_3N_4, respectively. Astonishingly, both the emission peaks were suppressed that inferred that the recombination of charged carriers was completely prevented.

All the characterization techniques results, especially the optical studies (UV-vis DRS and PL), indicate that Cu_2O–rGO–C_3N_4 can be a very good material for visible light active photocatalytic reactions. Therefore, photocatalytic reduction of 4-nitrophenol to 4-aminophenol was performed in presence of Cu_2O–rGO–C_3N_4 photocatalyst under visible light irradiation. For comparison, the photocatalytic reduction of 4-nitrophenol was performed using bare Cu_2O, rGO wrapped Cu_2O, pure C_3N_4, Cu_2O–C_3N_4, and Cu_2O–rGO–C_3N_4 (Figure 6). Among the photocatalysts used, bare Cu_2O showed lesser activity whereas the rGO wrapping increased the photocatalytic reduction property of Cu_2O. But the activity was comparatively lesser than the photocatalytic reduction of 4-nitrophenol using pristine C_3N_4. The photocatalytic activity of pristine C_3N_4 was increased slightly by loading bare Cu_2O (without rGO) spheres. However, the Cu_2O–rGO–C_3N_4 composite exhibited maximum reduction of 4-nitrophenol. This can be well explained by the fact that the recombination rate was

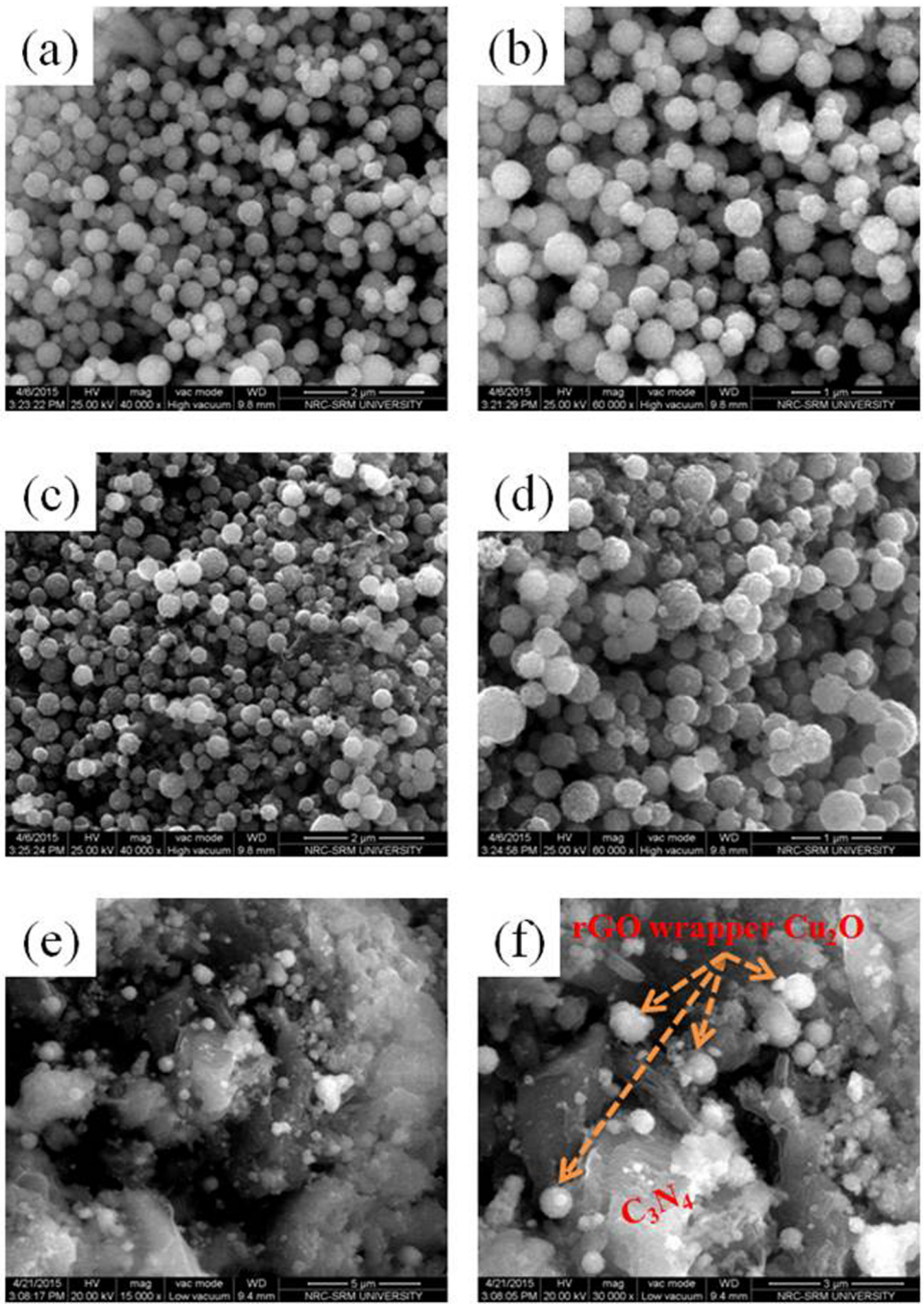

FIG. 4. SEM images of (a) and (b) APTES modified Cu_2O (c) and (d), rGO wrapped Cu_2O, and (e) and (f) Cu_2O–rGO–C_3N_4 composites.

completely prevented in Cu_2O–rGO–C_3N_4 photocatalyst as evident by the PL studies (Figure 5) and also that it possessed utmost visible light absorption capability as supported by the UV-vis DRS absorption spectrum [Figure S1(a) in the supplementary material].[36]

Based on the results, a tentative mechanism was proposed for the photocatalytic reduction of 4-nitrophenol using Cu_2O–rGO–C_3N_4 photocatalyst in presence of sodium sulfite under visible light irradiation (Figure 7). Both Cu_2O and C_3N_4 are visible light active photocatalysts and hence electron-hole pairs were generated in both the catalysts under visible light irradiation. The conduction band (CB) and valance band (VB) energy levels of Cu_2O are −0.7 V and 1.3 V, respectively.[30]

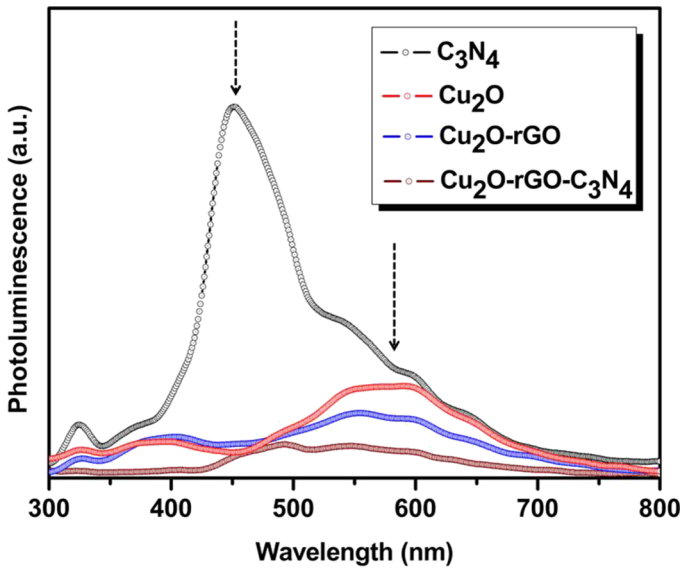

FIG. 5. Photoluminescence spectra of C_3N_4, Cu_2O, Cu_2O–rGO, and Cu_2O–rGO–C_3N_4 photocatalysts.

Since Cu_2O is a p-type semiconductor, the Fermi level energy is close to the VB.[31] On the other hand, the CB and VB potential of C_3N_4 are −1.13 V and 1.57 V, respectively.[32] But the Fermi level is nearer to the CB because it is an n-type semiconductor.[33] Apparently, the band structure of Cu_2O and C_3N_4 is not suitable for the formation of heterojunction. Nevertheless, when the rGO wrapped Cu_2O deposited on the surface of C_3N_4, the band structures were modified in such a way to reach the equilibrium between the Fermi levels of C_3N_4 and Cu_2O.[34] The negatively charged carriers move to the positive field (n-type C_3N_4) and the positive carriers migrate to the negative field (p-type Cu_2O). In other words, the CB of C_3N_4 behaved as a sink for the photogenerated electrons and subsequently the holes accumulated in the VB of Cu_2O.[35] Presence of rGO facilitated this carrier transport as strongly supported by the PL studies (Figure 5) and thereby increased the photocatalytic activity. The holes were utilized for the conversion of SO_3^{2-} to $SO_3^{\cdot-}$. On the other hand, the photoexcited electrons involved in the reduction of 4-nitrophenol to 4-aminophenol.

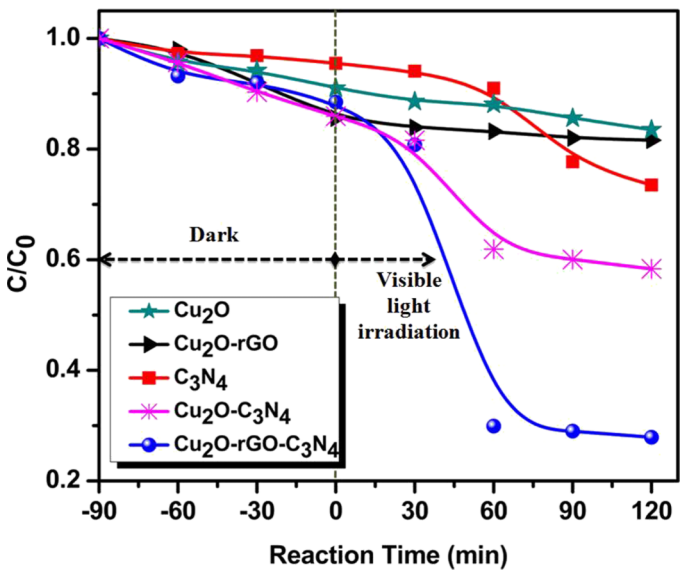

FIG. 6. Photocatalytic reduction of 4-nitrophenol to 4-aminophenol in presence of different photocatalysts.

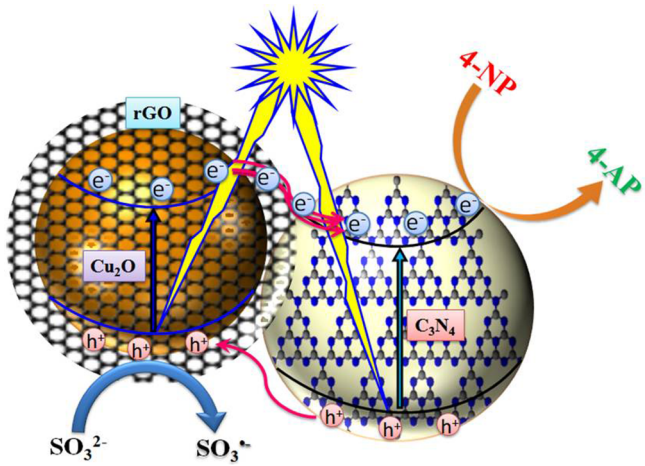

FIG. 7. Plausible mechanism for the photocatalytic reduction of 4-nitrophenol to 4-aminophenol using Cu_2O–rGO–C_3N_4 photocatalyst in presence of sodium sulfite.

In conclusion, rGO wrapped Cu_2O spheres were synthesized and loaded over C_3N_4 photocatalyst. By this synthetic route, the rGO was placed exactly at the interfacial of Cu_2O and C_3N_4 heterojunction and hence the photogenerated carrier migration became very rapid which was authenticated by the PL studies. As a result of this, the photocatalytic reduction ability of Cu_2O–rGO–C_3N_4 was enhanced ~2 fold synergistically as compared with that of the bare C_3N_4 and Cu_2O–rGO photocatalysts. A tentative mechanism was proposed for the reduction of 4-nitrophenol using Cu_2O–rGO–C_3N_4 photocatalyst under visible light irradiation. Photocatalyst recyclability was scrutinized for four times without any measurable loss in its photocatalytic activity.

We acknowledge financial support from the SERB (No. SR/FT/CS-127/2011), DST, New Delhi, India. We also acknowledge Professor B. Viswanathan, National Centre for Catalysis Research, IIT-Chennai for XPS analysis.

[1] P. V. Kamat, Chem. Rev. **93**, 267 (1993).
[2] S. Sakthivel, B. Neppolian, M. V. Shankar, B. Arabindoo, M. Palanichamy, and V. Murugesan, Sol. Energy Mater. Sol. Cells **77**, 65 (2003).
[3] J. Nisar, B. Pathak, and R. Ahuja, Appl. Phys. Lett. **100**, 181903 (2012).
[4] H. Yamashita, M. Harada, J. Misaka, M. Takeuchi, B. Neppolian, and M. Anpo, Catal. Today **84**, 191 (2003).
[5] A. L. Linsebigler, G. Lu, and J. T. Yates, Chem. Rev. **95**, 735 (1995).
[6] M. Suzuki, T. Ito, and Y. Taga, Appl. Phys. Lett. **78**, 3968 (2001).
[7] M. D. H. A. Fuerte, A. J. Maira, A. Martinez-Arias, M. Fernadez-Garcia, J. C. Conesa, and J. Soria, Chem. Commun. **24**, 2718 (2001).
[8] K. Takeuchi, I. Nakamura, O. Matsumoto, S. Sugihara, M. Ando, and T. Ihara, Chem. Lett. **29**, 1354 (2000).
[9] J. C. Yu, L. Zhang, Z. Zheng, and J. Zhao, Chem. Mater. **15**, 2280 (2003).
[10] T. Hirai, K. Suzuki, and I. Komasawa, J. Colloid Interface Sci. **244**, 262 (2001).
[11] D. Chatterjee and A. Mahata, Appl. Catal., B **33**, 119 (2001).
[12] J. Wang, T. Ma, G. Zhang, Z. Zhang, X. Zhang, Y. Jiang, G. Zhao, and P. Zhang, Catal. Commun. **8**, 607 (2007).
[13] X. Wang, K. Maeda, A. Thomas, K. Takanabe, G. Xin, J. M. Carlsson, K. Domen, and M. Antonietti, Nat. Mater. **8**, 76 (2009).
[14] Y. Wang, X. Wang, and M. Antonietti, Angew. Chem., Int. Ed. **51**, 68 (2012).
[15] S. C. Yan, S. B. Lv, Z. S. Li, and Z. G. Zou, Dalton Trans. **39**, 1488 (2010).
[16] S. Yan, Z. Li, and Z. Zou, Langmuir **26**, 3894 (2010).
[17] X. Li, J. Chen, X. Wang, J. Sun, and M. Antonietti, J. Am. Chem. Soc. **133**, 8074 (2011).
[18] L. F. Gou and C. J. Murphy, Nano Lett. **3**, 231 (2003).
[19] Y. Tian, B. Chang, J. Fu, B. Zhou, J. Liu, F. Xi, and X. Dong, J. Solid State Chem. **212**, 1 (2014).
[20] B. Neppolian, A. Bruno, C. L. Bianchi, and M. Ashokkumar, Ultrason. Sonochem. **19**, 9 (2012).
[21] S. G. Babu, R. Vinoth, D. P. Kumar, M. V. Shankar, H.-L. Chou, K. Vinodgopal, and B. Neppolian, Nanoscale **7**, 7849 (2015).
[22] S. G. Babu, R. Vinoth, B. Neppolian, D. D. Dionysiou, and M. Ashokkumar, J. Hazard. Mater. **291**, 83 (2015).
[23] S. G. Babu and R. Karvembu, Ind. Eng. Chem. Res. **50**, 9594 (2011).
[24] S. G. Babu, N. Neelakandeswari, N. Dharmaraj, S. D. Jackson, and R. Karvembu, RSC Adv. **3**, 7774 (2013).
[25] J. Zhu, Y. Wei, W. Chen, Z. Zhao, and A. Thomas, Chem. Commun. **46**, 6965 (2010).

[26] J. S. Lee, K. H. You, and C. B. Park, Adv. Mater. **24**, 1084 (2012).
[27] Y. Zhang, T. Mori, L. Niu, and J. Ye, Energy Environ. Sci. **4**, 4517 (2011).
[28] Y. Bai, T. Yang, Q. Gu, G. Cheng, and R. Zheng, Powder Technol. **227**, 35 (2012).
[29] J. Chen, S. Shen, P. Guo, M. Wang, P. Wu, X. Wang, and L. Guo, Appl. Catal., B **152–153**, 335 (2014).
[30] J. Zhang, J. Sun, K. Maeda, K. Domen, P. Liu, M. Antonietti, X. Fu, and X. Wang, Energy Environ. Sci. **4**, 675 (2011).
[31] A. Paracchino, V. Laporte, K. Sivula, M. Gratzel, and E. Thimsen, Nat. Mater. **10**, 456 (2011).
[32] L. Ge, C. Han, and J. Liu, Appl. Catal., B **108–109**, 100 (2011).
[33] P. Wang, Y. H. Ng, and R. Amal, Nanoscale **5**, 2952 (2013).
[34] Z. Zhang, C. Shao, X. Li, C. Wang, M. Zhang, and Y. Liu, ACS Appl. Mater. Interfaces **2**, 2915 (2010).
[35] J. Cao, X. Li, H. Lin, S. Chen, and X. Fu, J. Hazard. Mater. **239–240**, 316 (2012).
[36] See supplementary material at http://dx.doi.org/10.1063/1.4928286 for detailed experimental procedures for the preparation of materials, instrumental parameters and some of the results.